IOP Publishing Journal of Physics: Condensed Matter

J. Phys.: Condens. Matter **23** (2011) 055802 (7pp) doi:10.1088/0953-8984/23/5/055802

Generalized lucky-drift model for impact ionization in semiconductors with disorder

O Rubel, A Potvin and D Laughton

Thunder Bay Regional Research Institute, 290 Munro Street, Thunder Bay, ON, Canada
and
Lakehead University, 955 Oliver Road, Thunder Bay, ON, Canada

E-mail: rubelo@tbh.net

Received 9 November 2010, in final form 17 December 2010
Published 13 January 2011
Online at stacks.iop.org/JPhysCM/23/055802

Abstract

An extension of an original lucky-drift model to the case of disordered semiconductors is proposed, motivated by experimental observations of an avalanche phenomenon in amorphous semiconductors. The generalization encompasses two scattering mechanisms: an inelastic one due to optical phonons and an elastic one due to a disorder potential. An obtained analytical solution is verified by a kinetic Monte Carlo simulation. Eventually, experimental data on a field dependence of the impact ionization coefficient in amorphous selenium are interpreted using reasonable material parameters.

1. Introduction

In 1980 Juska and Arlauskas [1] pioneered the first clear experimental observation of impact ionization in an amorphous semiconductor (amorphous selenium, or a-Se), which was confirmed by further experimental studies [2, 3]. Due to these studies, the phenomenon of impact ionization in amorphous solids has found an application in photosensors for high-sensitivity TV camera tubes [2]. The combination of the unique photoconducting properties of a-Se with the impact ionization has a high potential in x- and γ-ray detectors for medical imaging applications [4, 5]. It is also believed that impact ionization is responsible for an electrical switching between the crystalline and amorphous phases in the chalcogenide alloys As_2Se_3 [6] and $Ge_2Sb_2Te_5$ [7, 8]. The latter topic is being actively investigated in the context of new-generation, non-volatile electronic data storage [9].

The theory of impact ionization in crystalline semiconductors is well established due to the fundamental contributions of Wolff [10], Shockley [11], Baraff [12] and Ridley [13]. The central point of the theory is finding a relation between the impact ionization coefficient, which is the inverse of the average distance traveled by a carrier prior to the ionization event, and the strength of the applied electric field. On its way, the carrier experiences energy and momentum relaxation scattering due to the interaction with phonons and/or defects that balances the energy gained by the carrier while drifting in the electric field.

Baraff [12] successfully solved the problem by computing numerically a free-carrier energy distribution function from the Boltzmann equation. Eventually, it turns out that neither Wolff's diffusion approximation [10] nor Shockley's lucky electron picture [11] is valid. The central assumptions of Baraff's theory are the following: (i) while drifting, electrons can gain energy only from the external electric field $\mathcal{E}$, (ii) electrons are subject to elastic scattering collisions characterized by an energy-independent mean free path λ_m, provided their kinetic energy does not exceed the optical phonon energy $\hbar\omega_{op}$, (iii) carriers with kinetic energy above $\hbar\omega_{op}$ undergo inelastic collisions only by emitting an optical phonon of the constant energy $\hbar\omega_{op}$ on the same mean free path, i.e., $\lambda_{op} = \lambda_m$, (iv) all scattering events are isotropic, (v) the impact ionization takes place immediately after the electron acquires the kinetic energy equal to the ionization threshold energy E_i. Despite the idealistic assumptions, Baraff's curves fit experimental data for the charge multiplication in crystalline semiconductors remarkably well [14]. As an alternative to the numerical Baraff curves, Ridley [13] suggested an analytical solution for the same problem known as a lucky-drift model. This model was further advanced by Burt [15] and tested against a kinetic Monte Carlo simulation [16]. No significant discrepancy was found between the simulation results and those of Baraff, Ridley, and Burt.

The development of a theory of impact ionization in amorphous solids was undertaken only recently. An attempt

to apply Shockley's theory to explain the field dependence of the impact ionization coefficient in a-Se failed, resulting in unrealistic material parameters [17]. Reasoning by Hindley [18] and the original lucky-drift mechanism proposed by Ridley [13] inspired the development of a modified lucky-drift model of avalanche in amorphous semiconductors proposed by Rubel *et al* [19] and Kasap *et al* [20]. The main feature of the modified lucky-drift model is an explicit treatment of elastic scattering due to the disorder potential inherent to amorphous solids, in addition to the inelastic scattering by optical phonons. The scattering by a disorder potential is assumed to be the dominant mechanism of the momentum relaxation for energetic electrons. The modified lucky-drift model contributed to resolving a long-standing question on the non-existence of avalanche in hydrogenated amorphous silicon [21]. The idea of applying the lucky-drift model to amorphous semiconductors received further attention in the work of Kasap *et al* [20]. Detailed analysis [22], however, revealed that the analytical formulation initially proposed in [19], and used so far, essentially underestimates the impact ionization coefficient.

The purpose of this communication is to extend an analytical formulation of the original lucky-drift model aiming at incorporating the effects of disorder on the carrier trajectory. These effects are associated with the intensive elastic scattering in addition to the inelastic optical phonon scattering as discussed previously in the context of the modified lucky-drift model [19]. The proposed analytical solution is thoroughly examined by comparison with results of a kinetic Monte Carlo simulation for the field dependence of the impact ionization coefficient. Finally, the obtained analytical expression for the field dependence of the impact ionization coefficient is applied to the interpretation of experimental data.

2. Model and simulation algorithm

The model studied here was originally proposed in [19] and, therefore, will only be briefly outlined for completeness. For avalanche multiplication to occur, the carriers must not be trapped either in shallow or deep traps and the trap-controlled transport [23] must become deactivated [24]. The simulations presented in this paper consider electronic device quality a-Se, in which the hole transport is not trap limited, that is the deep trap concentration is small [25], so that at sufficiently high fields the transport becomes deactivated.

We begin by assuming that, initially, a charge carrier is located at the origin of a coordinate system and has no kinetic energy. Under the influence of an applied electric field $\mathcal{E}$, the carrier begins to move in a direction prescribed by the field. Two independent scattering mechanisms influence the carrier trajectory: (i) elastic scattering by a disorder potential and acoustic phonons, (ii) inelastic scattering via emitting an optical phonon of energy $\hbar\omega_{\mathrm{op}}$. The elastic and inelastic scattering processes are characterized by associated individual mean free paths λ_{d} and λ_{op}, respectively. For the sake of simplicity, we neglect a possible anisotropy of the scattering angles and an energy dependence of λs. This assumption fully complies with Baraff's theory [12].

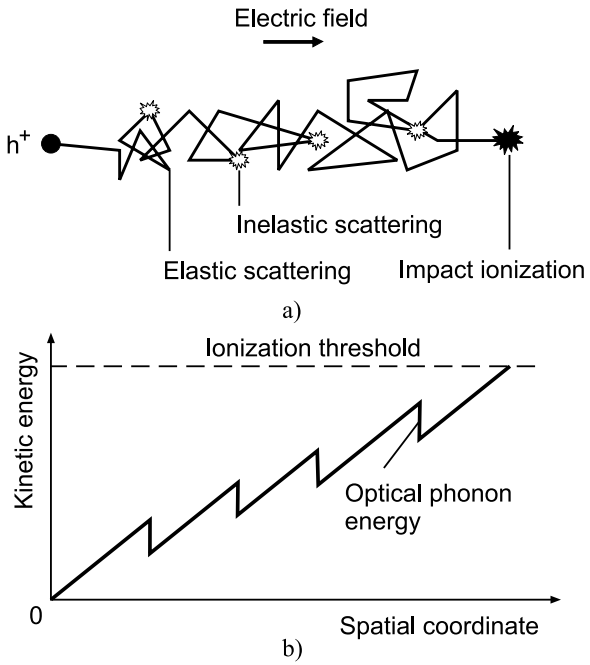

Figure 1. Carrier trajectory with relevant scattering processes (a) and the corresponding energy diagram (b).

The impact ionization takes place immediately after the carrier builds the kinetic energy equal to the ionization threshold E_{i}. The impact ionization coefficient is defined as [12]

$$\alpha = \langle Z \rangle^{-1}, \tag{1}$$

where $\langle Z \rangle$ is the average distance traveled by the carrier in the field direction prior to the ionization. Figure 1 illustrates schematically a typical carrier trajectory and the associated energy gain.

The simulation algorithm used here (figure 2) is similar in spirit to that described by Fawcett *et al* [26]. It employs a self-scattering approach [27], which introduces a fictitious 'forward' scattering in order to eliminate solving integral equations in every Monte Carlo step [28]. The self-scattering rate R_{ss} was taken to be the sum of the maximal elastic and inelastic scattering rates:

$$R_{\mathrm{ss}} = (\lambda_{\mathrm{d}}^{-1} + \lambda_{\mathrm{op}}^{-1})\sqrt{2E/m}. \tag{2}$$

Here m is the carrier effective mass and E is its kinetic energy. The stochastic free flight time $\mathrm{d}t$ is generated according to

$$\mathrm{d}t = -R_{\mathrm{ss}}^{-1} \ln(\xi), \tag{3}$$

where ξ is a random number with an even distribution between 0 and 1. The wavevector $\mathbf{k}$ of the change carriers and the position vector $\mathbf{x}$ associated with the free flight are determined by

$$\mathrm{d}\mathbf{k} = e\mathcal{E}\,\mathrm{d}t/\hbar \tag{4}$$

and

$$\mathrm{d}\mathbf{x} = \mathbf{k}\hbar\,\mathrm{d}t/m + e\mathcal{E}\,\mathrm{d}t^2/2m, \tag{5}$$

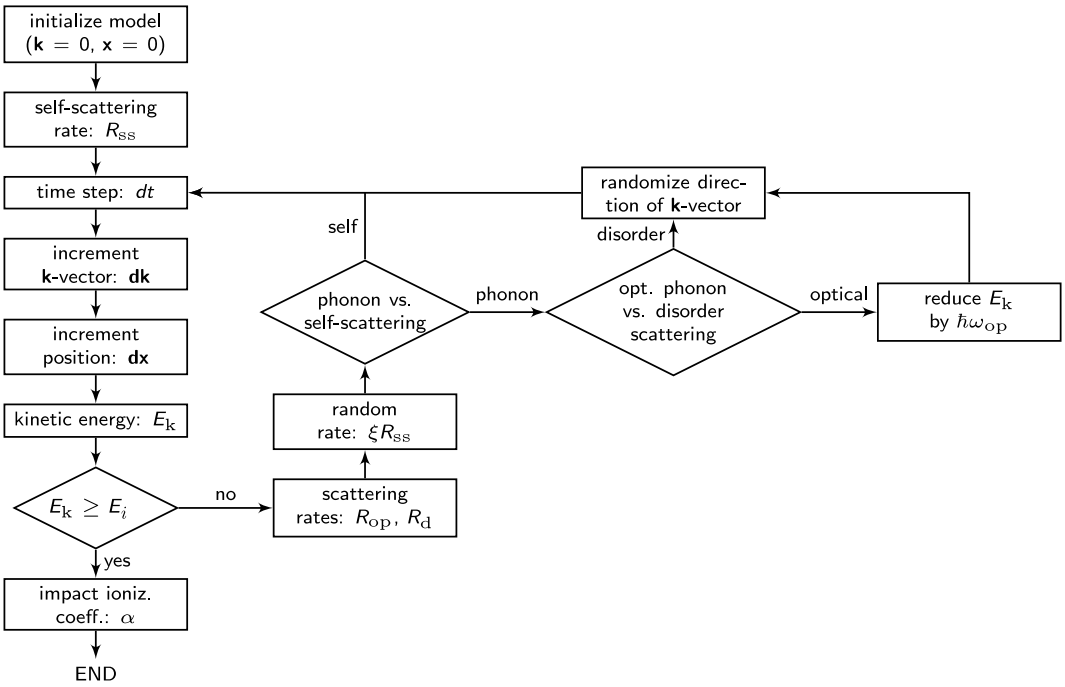

Figure 2. Simulation algorithm in the case of zero temperature.

respectively. Here e is a carrier charge and $\hbar$ is Plank's constant divided by 2π.

The elastic and inelastic scattering rates are calculated at the end of each free flight according to the following expression:

$$R = k\hbar/\lambda m. \tag{6}$$

The inelastic scattering rate is non-zero only if the kinetic energy $k^2\hbar^2/2m$ is equal to or greater than the optical phonon energy $\hbar\omega_{op}$.

The probability of elastic or inelastic scattering is determined by the ratio R/R_{ss}. Should one of these processes take place, we choose randomly a new orientation of the **k** vector and adjust its absolute value in the case of the inelastic scattering. If none of these processes occur, the carrier undergoes self-scattering, i.e., its **k** vector remains unchanged. After that, a new free flight time is generated according to equation (3), and the sequence is repeated until the carrier energy reaches the threshold E_i.

3. Results and discussion

3.1. Modification of the lucky-drift model

We begin with verification of the simulation algorithm by comparing its results with known analytical theories [12, 13, 16]. Since those theories imply scattering by optical phonons only, we temporarily eliminate elastic scattering from our model in order to enable a direct comparison. The simulation results are compared to the analytical solutions of Baraff [12], Ridley [13] and McKenzie and Burt [16] in figure 3. The agreement between our simulation and those analytical solutions gives confidence in the simulation algorithm.

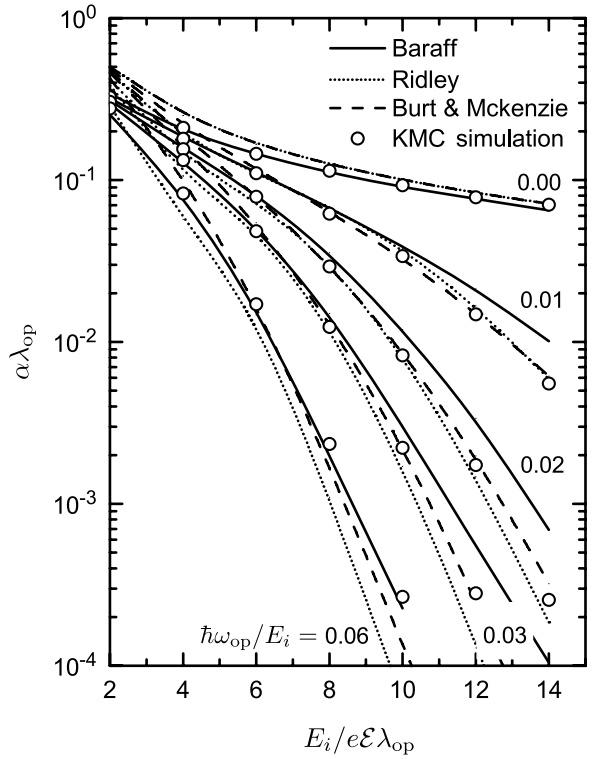

Figure 3. The impact ionization coefficient as a function of the electric field for various optical phonon energies. The analytical results shown by lines are due to Baraff [12], Ridley [13] and McKenzie and Burt [16]. The symbols are the results of the current kinetic Monte Carlo (KMC) simulation.

McKenzie and Burt's version of the lucky-drift model [16] provides, apparently, the most accurate analytical solution for the range of parameters selected in figure 3. In the

following, we extend the original lucky-drift model aiming at incorporating the effects of disorder on the carrier trajectory. These effects are associated with intensive elastic scattering in addition to the optical phonon scattering [19].

Our starting point is an expression for the impact ionization coefficient derived in the framework of a classical lucky-drift theory under the assumption of an energy-independent mean free path [16]:

$$\alpha\lambda_{\mathrm{m}} = \frac{\frac{\lambda_{\mathrm{m}}}{\lambda_E}\left[\exp\left(-\frac{l_0}{\lambda_E}\right) - \frac{\lambda_{\mathrm{m}}}{\lambda_E}\exp\left(-\frac{l_0}{\lambda_{\mathrm{m}}}\right)\right]}{1 - \exp\left(-\frac{l_0}{\lambda_E}\right) - \left(\frac{\lambda_{\mathrm{m}}}{\lambda_E}\right)^2\left[1 - \exp\left(-\frac{l_0}{\lambda_{\mathrm{m}}}\right)\right]}. \quad (7)$$

Here λ_{m} is the momentum relaxation mean free path, λ_E is the energy relaxation mean free path, and $l_0 = E_{\mathrm{i}}/e\mathcal{E}$ is the characteristic distance.

The energy relaxation mean free path λ_E is the central point of our modification. It is defined as the distance traveled by a carrier of energy E in the field direction prior to the full energy relaxation and can be expressed as

$$\lambda_E = v_{\mathrm{d}}(E)\tau_E(E), \quad (8)$$

where v_{d} is the drift velocity and τ_E is the energy relaxation time. The drift velocity is related to the momentum relaxation time τ_{m} via [13]

$$v_{\mathrm{d}}(E) = \frac{e\tau_{\mathrm{m}}(E)\mathcal{E}}{m}. \quad (9)$$

The energy relaxation time is simply a multiple of the optical phonon relaxation time, i.e., $\tau_E(E) = (E/\hbar\omega_{\mathrm{op}})\tau_{\mathrm{op}}(E)$.

In application to high-mobility semiconductors, the optical phonon scattering is considered as the dominant mechanism for both momentum and energy relaxation [12, 13, 16]. Thus, it is usually assumed that $\tau_{\mathrm{op}} = \tau_{\mathrm{m}}$. In our case, the disorder scattering is the dominant momentum relaxation mechanism, and the following inequality holds: $\tau_{\mathrm{op}} \gg \tau_{\mathrm{m}}$. In order to account for that feature, we introduce an additional parameter

$$\gamma = \lambda_{\mathrm{op}}/\lambda_{\mathrm{m}} = 1 + \lambda_{\mathrm{op}}/\lambda_{\mathrm{d}}, \quad (10)$$

which has appeared in previous studies [19, 21]. Then, the energy relaxation time can be expressed as

$$\tau_E(E) = \gamma\tau_{\mathrm{m}}(E)\frac{E}{\hbar\omega_{\mathrm{op}}}. \quad (11)$$

In the case of $\gamma = 1$, we recover the original lucky-drift model [13, 16], whereas $\gamma \gg 1$ corresponds to the modified lucky-drift model for amorphous solids [19].

Substituting equations (9) and (11) into (8), and taking into account that $E = mv_{\mathrm{g}}^2/2$ and $\lambda_{\mathrm{m}} = v_{\mathrm{g}}(E)\tau_{\mathrm{m}}(E)$, where v_{g} is the carrier group velocity, the expression for the energy relaxation mean free path takes the form

$$\lambda_E = \frac{e\gamma\lambda_{\mathrm{m}}^2\mathcal{E}}{2\hbar\omega_{\mathrm{op}}}. \quad (12)$$

Equations (7) and (12) yield to our main result: an expression for the impact ionization coefficient, which includes the effects of disorder:

$$\alpha\lambda_{\mathrm{m}} = \frac{\frac{2rx}{\gamma}\left[\exp\left(-\frac{2rx^2}{\gamma}\right) - \frac{2rx}{\gamma}\exp(-x)\right]}{1 - \exp\left(-\frac{2rx^2}{\gamma}\right) - \left(\frac{2rx}{\gamma}\right)^2[1 - \exp(-x)]}. \quad (13)$$

Here we use Ridley's notations: $x = E_{\mathrm{i}}/e\mathcal{E}\lambda_{\mathrm{m}}$ and $r = \hbar\omega_{\mathrm{op}}/E_{\mathrm{i}}$. This result shows that two independent scattering processes—elastic by the disorder potential and inelastic by optical phonons—can be viewed as a single inelastic scattering process characterized by an effective energy $\hbar\omega_{\mathrm{op}}/\gamma$ emitted per collision and by the reduced mean free path λ_{m} determined by equation (10).

3.2. Comparison with simulation

Before we begin a comparison between the proposed analytical expression for the impact ionization coefficient and simulation results, we need to identify a range of parameters relevant for a-Se. Following Hindley [18], we assume that the ionization threshold energy E_{i} in disordered semiconductors equals their mobility gap. The latter is about $2.1 \cdots 2.3$ eV in a-Se [24, 29]. The optical phonon spectrum is centered at 31 meV [30], which results in $\hbar\omega_{\mathrm{op}}/E_{\mathrm{i}} \approx 0.014$.

Amorphous selenium features a relatively low microscopic hole mobility of about 1 cm^2 V^{-1} s^{-1}, even for substantially hot carriers [1]. In a relaxation time approximation, such a value of the drift mobility corresponds to the mean free path of the order of an interatomic spacing; therefore, we assume $\lambda_{\mathrm{m}} \sim 0.5$ nm. Taking into account this value and the magnitude of electric field $\mathcal{E} = 0.75 \cdots 1.70$ MV cm^{-1} at which the impact ionization is observed in a-Se, we determine the range for another parameter $E_{\mathrm{i}}/e\mathcal{E}\lambda_{\mathrm{m}} = 30 \cdots 70$.

The mean free path due to the optical phonon scattering, λ_{op}, in semiconductors is typically of the order of tens of angstroms [31]. Ridley [31] proposed a simple empirical expression $\lambda_{\mathrm{op}}[\mathrm{nm}] \sim 60\rho\hbar\omega_{\mathrm{op}}E_{\mathrm{i}}^{-1/2}$ which relates the optical phonon mean free path to the material density ρ, the optical phonon frequency, and the ionization energy. Taking $\rho = 4.3$ g cm^{-3} ([32], p 129) and $\hbar\omega_{\mathrm{op}} = 0.031$ eV [21], we obtain $\lambda_{\mathrm{op}} \sim 5$ nm in a-Se. This value is comparable with the inelastic scattering length of approximately 3 nm deduced by Juska [24]. Eventually, it is possible to identify the ratio $\lambda_{\mathrm{op}}/\lambda_{\mathrm{m}} = 10^{+10}_{-5}$. The uncertainty reflects an inaccuracy in estimates for the mean free paths.

Values of the impact ionization coefficient calculated using the generalized lucky-drift model (equation (13)) are compared with results of the kinetic Monte Carlo simulation in figure 4(a). The analytical results match well with the simulation data for the selected range of parameters, which confirms the confidence of our extension to the lucky-drift model. Analytical results obtained using the previous mathematical expression [19] for the field dependence of the impact ionization coefficient are also shown in figure 4(a). The comparison clearly indicates that equation (13) is much more accurate than the former analytical solution [19].

In the limit of $\lambda_E \gg \lambda_{\mathrm{m}}$ and $l_0 \gg \lambda_E$, which is relevant in our case, equation (7) can be reduced to [16]

$$\alpha \approx \lambda_E^{-1}(\mathcal{E})\exp\left[-\frac{E_{\mathrm{i}}}{e\mathcal{E}\lambda_E(\mathcal{E})}\right]. \quad (14)$$

This result resembles Shockley's ballistic expression [11] for the impact ionization coefficient, though using λ_E instead of λ_{m} [16]. We confirm the validity of equation (14) by re-plotting

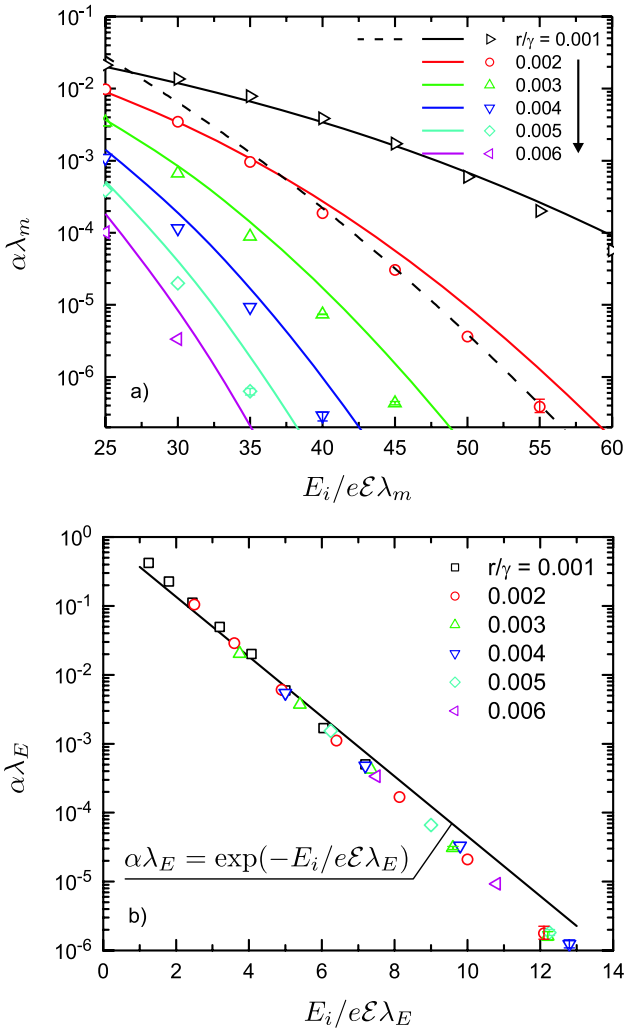

Figure 4. The impact ionization coefficient as a function of the electric field for various r/γ ratios. The symbols are the results of the current kinetic Monte Carlo simulation. The solid lines in panel (a) represent the analytical results of equation (13); the dashed line corresponds to the analytical solution proposed in [19] (shown only for $r/\gamma = 0.001$). Panel (b) represents the same simulation data as in panel (a) using the energy relaxation mean free path defined by equation (12) instead of the momentum relaxation mean free path for normalization. The line in panel (b) corresponds to the approximate expression for the impact ionization coefficient. The error bars are ±5%, unless otherwise indicated.

(This figure is in colour only in the electronic version)

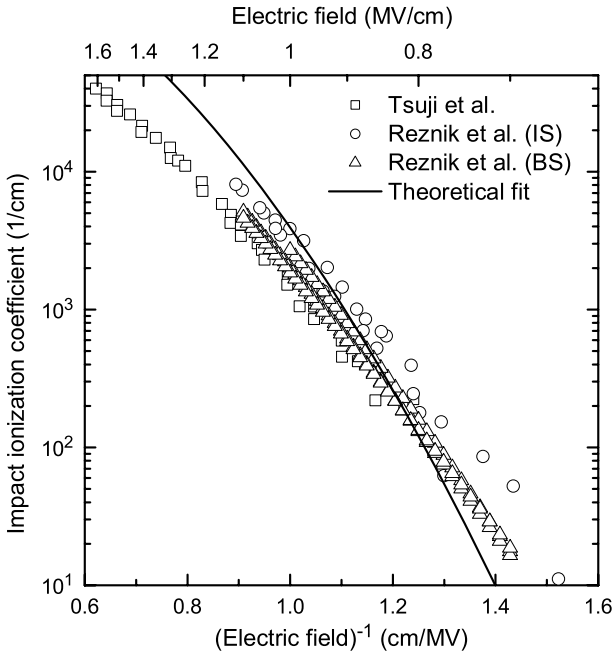

Figure 5. The impact ionization coefficient as a function of the electric field in a-Se. The symbols represent the experimental data reported by Tsuji *et al* [3] and Reznik *et al* [21]. IS and BS refer to an insulating and blocking structure, respectively. The solid line corresponds to the best fit to the experimental data using equation (14) with the parameters listed in table 1.

the simulation data in figure 4(b) using λ_E as a normalization factor for distances on both coordinates axes. As a result, the simulation data from figure 4(a) merge into a single line, which fits to equation (14) as shown in figure 4(b). This asymptotic form has an important advantage; namely, it allows us to reduce the number of independent fitting parameters down to two arguments: E_i and $\lambda_\mathrm{op}\lambda_\mathrm{m}/\hbar\omega_\mathrm{op}$. Below, we attempt to extract these parameters by fitting equation (14) to experimental data.

3.3. Comparison with experiment

Experimental data for the field dependence of the impact ionization coefficient in a-Se adopted from [3, 21] are gathered in figure 5. These data are fitted to equation (14) using the fixed ionization threshold energy $E_\mathrm{i} = 2.3$ eV and only one adjustable parameter $\lambda_\mathrm{op}\lambda_\mathrm{m}/\hbar\omega_\mathrm{op}$. The corresponding best-fit curve is shown in figure 5.

The extracted value of the material parameter $\lambda_\mathrm{op}\lambda_\mathrm{m}/\hbar\omega_\mathrm{op}$ is 70 nm^2 eV^{-1}. Taking $\hbar\omega_\mathrm{op} = 31$ meV for the optical phonon frequency in a-Se [21] and implying the momentum relaxation mean free path of 0.5 nm, we deduce the optical phonon mean free path of 4.3 nm. (Also note that the uncertainty in λ_op is directly related to the uncertainty in λ_m, since only their product matters.) The found value of λ_op agrees well with the estimate made above.

The value of the optical phonon mean free path found from the fit to the experimental data for a-Se using a less accurate mathematical formulation [19, 21] has a discrepancy of nearly a factor of two, when compared to the value extracted using equation (14). The reason for such a discrepancy is neglect of the drift contribution to the carrier trajectory in [19], which leads to an underestimate of the impact ionization rate [22]. The analytical expression presented here overcomes that deficiency. This improvement is crucial for quantitative analysis of experimental data.

We would like to emphasize that the theoretical model presented here contains the *minimal* set of parameters (table 1) required in order to capture the essence of hot carrier transport in a disordered semiconductor. It is apparent from figure 5 that the theory predicts a stronger dependence of the impact ionization coefficient on the electric field than that observed experimentally. In order to align the theoretical curve with the experimental data, one has to assume either an unreasonably

Table 1. The parameters used in the theoretical fit to the experimental data in figure 5 for a field dependence of the impact ionization coefficient in a-Se.

Parameter	Symbol	Units	Value
Momentum relaxation mean free path	λ_m	nm	0.5
Optical phonon mean free path	λ_{op}	nm	4.3
Ionization threshold energy	E_i	eV	2.3
Optical phonon energy	$\hbar\omega_{op}$	meV	31

large ionization threshold energy $E_i \sim 13$ eV or some field/energy dependence of the λs. Recent calculations [33] of the volume deformation potential and its energy dependence in selenium clearly favor the latter assumption. These scenarios were thoroughly investigated by Kasap *et al* [20], though in the framework of the original lucky-drift model. However, extension of the generalized lucky-drift model to the case of energy-dependent mean free paths and its verification by a kinetic Monte Carlo simulation is beyond the scope of this paper.

Further improvement of the theory can be achieved by taking into account the energy dependence of the impact ionization rate, i.e., by introducing a 'soft' ionization threshold. This dependence includes details of the band structure and varies significantly for different semiconductors [34]. In the absence of any information in the literature on the energy dependence of the impact ionization rate for charge carriers in a-Se, we can only qualitatively describe the anticipated effect of the soft threshold on the field dependence of the impact ionization coefficient. Implementation of the soft threshold would lead to an increase of the effective ionization threshold energy, which requires a corresponding adjustment of the $\lambda_{op}\lambda_m$ product. As a consequence, one can expect a weaker field dependence of the impact ionization coefficient, according to the arguments presented in the preceding paragraph, resulting in a better fit to the experimental data.

Finally, we comment on the temperature dependence of the impact ionization coefficient in a-Se. In contrast to crystalline semiconductors, which typically feature a decrease of the impact ionization coefficient with increasing temperature, the measurements of Tsuji *et al* [3] revealed a positive temperature dependence of both the hole and electron impact ionization coefficients in a-Se. In the framework of the chosen model, the temperature affects only the optical phonon scattering by alternation of the phonon population. The simulation shows that, at the electric field of 1 MV cm^{-1}, the temperature variation in the range $0 \cdots 300$ K has no significant effect on the impact ionization coefficient within a 5% error bar. This result is well justified giving that $k_B T < \hbar\omega_{op}$, where k_B is the Boltzmann constant. Therefore, the positive temperature dependence of the impact ionization coefficient in a-Se comes from effects that are not captured within our model. Possible candidates include (i) the temperature enhanced electron–hole pair dissociation [3], (ii) the thermal activation of secondary generated charge carriers from shallow localized states [20], and (iii) the temperature dependence of the impact ionization threshold [35]. However, it is problematic to justify mechanisms (i) and (ii) in the light of the soft ionization threshold, since secondary carriers will likely have a non-zero kinetic energy.

4. Conclusions

The dependence of the impact ionization coefficient on the applied electric field in disordered semiconductors was studied theoretically. The simplest model was considered, which features an inelastic scattering of charge carriers due to their interaction with optical phonons mediated by an intensive elastic scattering on a disorder potential. An analytical solution for the formulated problem was obtained as an extension of the original lucky-drift model proposed by Ridley [13] and Burt [15]. It was shown that the two scattering mechanisms inherent to disordered semiconductors can be combined into a single inelastic scattering process characterized by an effective energy loss per collision and by a reduced mean free path. A kinetic Monte Carlo simulation was performed in order to verify the analytical formulation, which turns out to be much more accurate than the expression previously suggested in [19]. Experimental data for the field dependence of the impact ionization coefficient in amorphous selenium were fitted by the proposed expression using a reasonable set of material parameters. The extracted value of the optical phonon mean free path was found in agreement with independent estimates.

Acknowledgments

The authors are indebted to S D Baranovskii and A Reznik for stimulating discussions. Financial support of the Natural Sciences and Engineering Research Council of Canada under a Discovery Grants Program 'Microscopic theory of high-field transport in disordered semiconductors', the Ontario Ministry of Research and Innovation through a Research Excellence Program 'Ontario network for advanced medical imaging detectors', and the Thunder Bay Regional Health Sciences Foundation is gratefully acknowledged.

References

[1] Juska G and Arlauskas K 1980 *Phys. Status Solidi* a **59** 389
[2] Tanioka K, Yamazaki J, Shidara K, Taketoshi K, Kawamura T, Ishioka S and Takasaki Y 1987 *IEEE Electron Device Lett.* **8** 392
[3] Tsuji K, Takasaki Y, Hirai T and Taketoshi K 1989 *J. Non-Cryst. Solids* **114** 94
[4] Reznik A, Baranovskii S D, Rubel O, Jandieri K, Kasap S, Ohkawa Y, Kubota M, Tanioka K and Rowlands J 2008 *J. Non-Cryst. Solids* **354** 2691
[5] Kasap S, Frey J B, Belev G, Tousignant O, Mani H, Laperriere L, Reznik A and Rowlands J A 2009 *Phys. Status Solidi* b **246** 1794
[6] Hindley N K 1970 *J. Non-Cryst. Solids* **5** 31
[7] Pirovano A, Lacaita A L, Benvenuti A, Pellizzer F and Bez R 2004 *IEEE Trans. Electron Devices* **51** 452
[8] Jandieri K, Rubel O, Baranovskii S D, Reznik A, Rowlands J A and Kasap S O 2009 *J. Mater. Sci., Mater. Electron.* **20** S221
[9] Wuttig M and Yamada N 2007 *Nat. Mater.* **6** 824
[10] Wolff P A 1954 *Phys. Rev.* **95** 1415
[11] Shockley W 1961 *Solid-State Electron.* **2** 35 (ISSN 0038-1101)
[12] Baraff G A 1962 *Phys. Rev.* **128** 2507
[13] Ridley B K 1983 *J. Phys. C: Solid State Phys.* **16** 3373

[14] Ghynoweth A G 1968 *Semiconductors and Semimetals: Physics of III–V Compounds* vol 4 (London: Academic) chapter (Charge Multiplication Phenomena) pp 263–326
[15] Burt M G 1985 *J. Phys. C: Solid State Phys.* **18** L477
[16] McKenzie S and Burt M G 1986 *J. Phys. C: Solid State Phys.* **19** 1959
[17] Arkhipov V I and Kasap S O 2000 *J. Non-Cryst. Solids* **266** 959
[18] Hindley N 1972 *J. Non-Cryst. Solids* **8–10** 557
[19] Rubel O, Baranovskii S D, Zvyagin I P, Thomas P and Kasap S O 2004 *Phys. Status Solidi* c **1** 1186
[20] Kasap S, Rowlands J A, Baranovskii S D and Tanioka K 2004 *J. Appl. Phys.* **96** 2037
[21] Reznik A, Baranovskii S D, Rubel O, Juska G, Kasap S O, Ohkawa Y, Tanioka K and Rowlands J A 2007 *J. Appl. Phys.* **102** 053711
[22] Jandieri K, Rubel O, Baranovskii S, Reznik A, Rowlands J and Kasap S 2008 *J. Non-Cryst. Solids* **354** 2657 (ISSN 0022-3093)
[23] Kasap S O, Polischuk B and Dodds D 1990 *Rev. Sci. Instrum.* **61** 2080
[24] Juska G 1991 *J. Non-Cryst. Solids* **137/138** 401
[25] Kasap S and Juhasz C 1982 *Photogr. Sci. Eng.* **26** 239
[26] Fawcett W, Boardman A D and Swain S 1970 *J. Phys. Chem. Solids* **31** 1963
[27] Rees H D 1969 *J. Phys. Chem. Solids* **30** 643
[28] Jacoboni C and Reggiani L 1983 *Rev. Mod. Phys.* **55** 645
[29] Davis E 1970 *J. Non-Cryst. Solids* **4** 107
[30] Carroll P J and Lannin J S 1981 *Solid State Commun.* **40** 81 (ISSN 0038-1098)
[31] Ridley B K 1983 *J. Phys. C: Solid State Phys.* **16** 4733
[32] Popescu M A 2000 *Non-Crystalline Chalcogenicides* (Dordrecht: Kluwer Academic)
[33] Rubel O and Laughton D 2010 *J. Phys.: Condens. Matter* **22** 355803
[34] Bude J and Hess K 1992 *J. Appl. Phys.* **72** 3554
[35] Waldron N, Pitera A, Lee M, Fitzgerald E and del Alamo J 2005 *IEEE Trans. Electron Devices* **52** 1627